Skin microdialysis detects distinct immunological patterns in chronic inflammatory skin diseases

Moritz Maximilian Hollstein, MD, Stephan Traidl, MD, Anne Heetfeld, MD, Susann Forkel, MD, Andreas Leha, PhD, Natalia Alkon, PhD, Jannik Ruwisch, MD, Christof Lenz, PhD, Michael Peter Schön, MD, Martin Schmelz, MD, Patrick Brunner, MD, MSc, Martin Steinhoff, MD, PhD, Timo Buhl, MD

PII: S0091-6749(24)00782-6

DOI: https://doi.org/10.1016/j.jaci.2024.06.024

Reference: YMAI 16444

To appear in: *Journal of Allergy and Clinical Immunology*

Received Date: 4 December 2023

Revised Date: 24 April 2024

Accepted Date: 4 June 2024

Please cite this article as: Hollstein MM, Traidl S, Heetfeld A, Forkel S, Leha A, Alkon N, Ruwisch J, Lenz C, Schön MP, Schmelz M, Brunner P, Steinhoff M, Buhl T, Skin microdialysis detects distinct immunological patterns in chronic inflammatory skin diseases, *Journal of Allergy and Clinical Immunology* (2024), doi: https://doi.org/10.1016/j.jaci.2024.06.024.

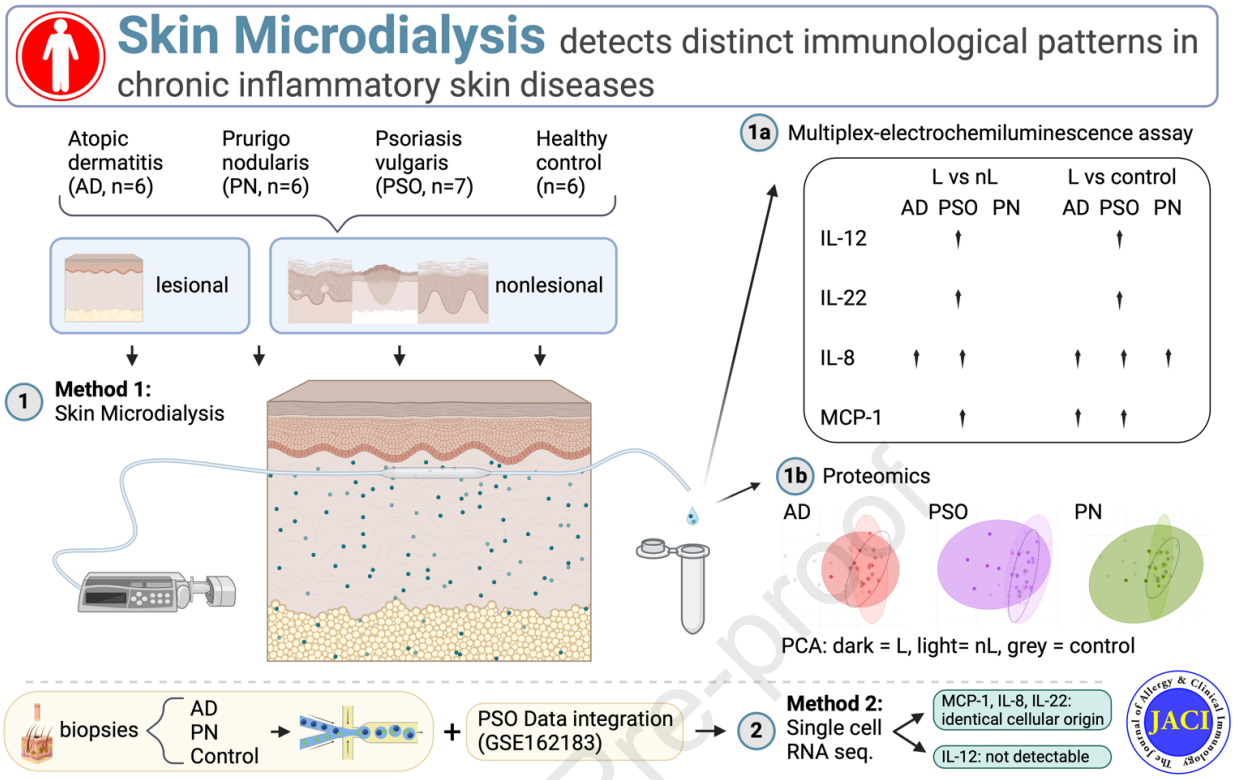

Skin microdialysis detects distinct immunological patterns in chronic inflammatory skin diseases

Moritz Maximilian Hollstein, MD[1], Stephan Traidl, MD[2], Anne Heetfeld, MD[1], Susann Forkel, MD[1], Andreas Leha, PhD[3], Natalia Alkon, PhD[4], Jannik Ruwisch, MD[5], Christof Lenz, PhD[6,7], Michael Peter Schön, MD[1], Martin Schmelz, MD[8], Patrick Brunner, MD, MSc[9], Martin Steinhoff, MD, PhD[10], Timo Buhl, MD[1]

[1] Department of Dermatology, Venereology and Allergology, University Medical Centre Göttingen, Göttingen, Germany

[2] Department of Dermatology and Allergy, Hannover Medical School, Hannover, Germany

[3] Department of Medical Statistics, University Medical Center Göttingen, Germany

[4] Department of Dermatology, Medical University of Vienna, Vienna, Austria

[5] Clinic for Respiratory Medicine, Hannover Medical School, Hannover, Germany

[6] Department of Clinical Chemistry, UMG, Göttingen, Germany

[7] Bioanalytical Mass Spectrometry, Max Planck Institute for Multidisciplinary Sciences, Göttingen, Germany

[8] Department of Experimental Pain Research, MCTN, Medical Faculty Mannheim, University of Heidelberg, Mannheim, Germany

[9] Department of Dermatology, Icahn School of Medicine at Mount Sinai, New York, USA

[10] Department of Dermatology and Venereology, Hamad Medical Corporation, Doha, Qatar

Short Title: Microdialysis of inflammatory skin

Keywords: Microdialysis, Pruritus, Atopic Dermatitis, Psoriasis vulgaris

Abbreviations:

AD:	Atopic Dermatitis
COL1A1:	Alpha-1 Type I Collagen
DLQI:	Dermatology Life Quality Index
EASI:	Eczema Area and Severity Index
FABP:	Fatty Acid Binding Protein
GO:	Gene Ontology
IFN:	Interferon
IL:	Interleukin
KEGG:	Kyoto Encyclopedia of Genes and Genomes
OSBPL1A:	Oxysterol Binding Protein Like 1A
PASI:	Psoriasis Area and Severity Index
PCA:	Principal Component Analysis
PN:	Prurigo Nodularis
PSO:	Psoriasis Vulgaris
TSLP:	Thymic Stromal Lymphopoietin
UMAP:	Uniform Manifold Approximation and Projection

Key Messages

- Microdialysis can be used to analyze inflammatory skin diseases.
- Microdialysate can be analyzed using -omics or high-sensitivity (multiplex) ELISA.

- In PN and PSO, inflammation may be limited to lesional skin, whereas in AD, nonlesional skin shows characteristics of lesional skin.

Corresponding Author:

Moritz Hollstein, MD

University Medical Center Göttingen

Department of Dermatology, Venereology and Allergology

Robert Koch Str. 40

37075 Göttingen, Germany

Email: moritz.hollstein(at)med.uni-goettingen.de

Word count: 4451, 1 table, 5 figures, supplement

Statement of Ethics

The research was conducted ethically in accordance with the World Medical Association Declaration of Helsinki.

Study Approval Statement

This study was reviewed and approved by the UMG ethics committee prior to study implementation (approval number 31/11/17).

Consent to Participate Statement

All participants provided written informed consent.

Conflict of Interest Statement

The authors have no conflicts of interest to declare.

Funding Sources

Funding was partly granted by Kiniksa (San Diego, USA) and a scholarship from the Deutsche Forschungsgemeinschaft (DFG) – 413501650 (to MMH).

Author Contributions

Contributions: SF, MS and TB designed the study. AH, SF, ST, CL, PB, NA and MMH collected data. Cl, ST and MMH extracted and compiled data. All authors discussed data. ST

and MMH drafted the manuscript. All authors jointly discussed, reviewed and amended the manuscript. Data verification was performed by AL, CL, MMH, ST, MS and TB.

Data Availability Statement

Datasets are available here: https://www.ebi.ac.uk/pride/archive/projects/PXD050245

Abstract (200–250 words)

Background:

Insight into the pathophysiology of inflammatory skin diseases, especially at the proteomic level, is severely hampered by the lack of adequate in situ data.

Objective:

Characterize lesional and nonlesional skin of inflammatory skin diseases using skin microdialysis.

Methods:

Skin microdialysis samples from patients with atopic dermatitis (AD, n=6), psoriasis vulgaris (PSO, n=7) or prurigo nodularis (PN, n=6), as well as healthy controls (n=7) were subjected to proteomics and multiplex cytokine analysis. Single-cell RNA sequencing of skin biopsy specimens was used to identify the cellular origin of cytokines.

Results:

Among the top 20 enriched GO annotations, NAD metabolic process, regulation of secretion by cell, and pyruvate metabolic process were elevated in microdialysates from lesional AD skin compared with both nonlesional skin and controls. The top 20 enriched KEGG pathways in these three groups overlapped almost completely. In contrast, nonlesional skin from patients with PSO or PN and control skin showed no overlap with lesional skin in this KEGG pathway analysis. Lesional skin from patients with PSO, but not AD or PN, showed significantly elevated protein levels of MCP-1 compared to nonlesional skin. IL-8 was elevated in lesional vs nonlesional AD and PSO skin, whereas IL-12p40 and IL-22 were higher only in lesional

PSO skin. Integrated single-cell RNA-seq data revealed identical cellular sources of these cytokines in AD, PSO and PN.

Conclusion:

Based on microdialysate, proteomic data of lesional PSO and PN skin, but not lesional AD skin, differed significantly from those of nonlesional skin. IL-8, IL-22, MCP-1 and IL-12p40 might be suitable markers for minimally invasive molecular profiling.

Capsule Summary

This study proves skin microdialysis is a valuable tool to analyze inflammatory skin lesions and shows that in atopic dermatitis, contrary to psoriasis vulgaris and prurigo nodularis, nonlesional skin shows characteristics of lesional skin.

Introduction

Autoimmune and inflammatory skin disorders are noninfectious diseases with a complex immune-mediated pathophysiology.[1] One method to classify these diseases is based on cytokine profiles and T helper cell involvement. Type 1 immune responses may induce keratinocyte necroptosis in an interferon (IFN)-y-dependent manner in certain autoimmune diseases, such as lupus erythematosus or lichen planus.[1] The physiological role of this type of immune responses may involve defense against intracellular bacteria and protozoa, as well as viruses.[2] Type 2 immune responses induce IgE-producing plasma cells and pruritus, the latter via cytokines such as interleukin (IL)-31.[3,4] They are important for venom neutralization, protection against parasites, tissue repair and tissue fibrosis; these responses play critical roles in allergic diseases such as atopic dermatitis (AD).[2,5,6] Type 3 immune responses are mediated primarily by IL-22, IL-17A and IL-17F.[2] These cytokines mediate epidermal proliferation (acanthosis), recruitment of neutrophils and antimicrobial peptide synthesis.[2] These mechanisms aid in defense against extracellular bacteria and fungi. Type 3 immune responses are also involved in the pathogenesis of psoriasis vulgaris (PSO).[7] Assessing lesional cytokine profiles is difficult through conventional diagnostics such as histopathologic classification of lesional skin including immune cell infiltrates. Thus, although cytokine profiles are used in basic research, they do not aid routine diagnostics.

Furthermore, for some diseases such as AD, several endotypes have been proposed that cannot be distinguished by conventional diagnostics.[8] In PSO and AD, overlapping phenotypes have been described, thus resulting in misdiagnosis; these phenotypes are sometimes referred to as psoriasiform eczema, eczematous PSO or sebopsoriasis.[9,10] Furthermore, in AD, nonlesional skin shares many characteristics with lesional skin, such as barrier defects and T cell infiltrates, and can be as pruritic as lesional skin.[9-11] Thus, an improved minimally invasive toolbox would be very desirable to detect inflammatory patterns for more accurate diagnosis.

Current options to characterize inflammatory skin diseases are based on molecular disease classifiers at the genetic level or through omics.[14,15] These procedures generally require skin biopsies and are time-consuming and costly. We hypothesized that classification and diagnosis of inflammatory skin diseases might be performed on the basis of protein expression rather than genetic or transcriptomic analyses. We further hypothesized that quantifying individual proteins (including cytokines and chemokines) as well as other soluble components in the intercellular space might enable disease profiling, thus allowing invasive skin biopsies to be avoided in the future.

To collect samples for minimally invasive extracellular protein-analysis, we performed microdialysis of the skin. The procedure involves penetrating the patient's dermis with a semipermeable polycarbonate membrane and subsequent perfusion. Relevant soluble components penetrate through pores into the dialysate.[14-16] Microdialysis causes little pain, leaves no scar, and can be repeated in the same location, in contrast to punch biopsies of the skin. We demonstrate the feasibility of skin microdialysis as a minimally invasive diagnostic tool for profiling the inflammatory skin diseases AD, PSO, and prurigo nodularis (PN). Furthermore, by comparing lesional with non-lesional skin of patients and with skin of healthy controls, we propose disease markers (cytokines and chemokines) locally at the protein level.

Patients and Methods

After obtaining informed consent, we performed skin microdialysis on 26 volunteers with AD (n=6), PSO (n=7) or PN (n=6), and healthy controls (n=7). Additional patient samples of three patients with prurigo simplex subacuta were used for generating the proteomics library. The Eczema Area and Severity Index (EASI) was determined for all patients with AD, and the Psoriasis Area and Severity Index (PASI) was determined for all patients with PSO before the microdialysis procedure. In all patients, Dermatology Life Quality Index (DLQI) was evaluated, and pruritus was assessed on an 11-point Visual Analogue Scale. This study was conducted in accordance with the World Medical Association Declaration of Helsinki and reviewed and approved by the local ethics committee, approval number 31/11/17.

Skin microdialysis

The microdialysis procedure was performed as previously described.[16] Catheter tubes were custom-made in the laboratory of MSc. Catheters were hollow fibers (0.4 mm in diameter with a pore-size cut-off of 3,000 kDa). Patients were seated in a comfortable position in a temperature- and humidity-controlled environment for at least 20 minutes before the start of the procedure (Figure S1A). Subsequently, a 25-gauge cannula connected to the hollow fiber and an attached flexible tube were prepared in a germ-reduced environment (Figure S1B). The cannula was inserted intradermally over a distance of 1 cm at the area of interest located on an extremity, primarily the upper arm (lesional skin; nonlesional skin, i.e., skin without visible lesions; or skin of healthy controls) (Figure S1C, D) and the attached hollow fiber was threaded through the skin. This procedure was generally well tolerated, and no local anesthesia was required. The correct intracutaneous positioning of the catheter was verified, and the needle was detached from the catheter by cutting the catheter at the outflow side (Figure S2A). Ringer's solution (B. Braun SE, Melsungen, Göttingen) was perfused at a rate of 5 µl/min with

a syringe pump (CMA 4004, Harvard Apparatus, USA) via a Tygon tube (Novodirekt, Kehl, Germany). A microcentrifuge tube (1.5 ml) was positioned just below the loose end of the catheter to collect the dialysate (Figure S2B). In the 40-minute sampling period, two dialysate samples were collected, one every 20 minutes.

Proteomics mass spectrometry sample preparation

For proteomics analysis, samples from six patients with AD, seven patients with PSO, four patients with PN and seven healthy controls were available. Two samples from patients with PN could not be included because of technical issues. For each disease, lesional and nonlesional dialysates were evaluated in technical duplicates. Proteins were extracted, purified and digested with tryptase according to a magnetic bead-based SP3 protocol.[19] Digested peptides were dried in a SpeedVac instrument and stored at -20°C until further analysis. For generation of a peptide library, equal aliquots from each sample were pooled to a total amount of 200 µg and separated into 12 fractions with basic pH reverse phase C18 separation on an FPLC system (äkta pure, Cytiva, Marlborough, MA, USA) with a 36/3 staggered pooling scheme. All samples were spiked with a synthetic peptide standard used for retention time alignment (iRT Standard, Schlieren, Switzerland).

Protein digests were analyzed on a nanoflow chromatography system (Eksigent nanoLC425) connected to a hybrid triple quadrupole-TOF mass spectrometer (TripleTOF 5600+) equipped with a Nanospray III ion source (ion spray voltage 2400 V; interface heater temperature 150°C; sheath gas setting 12) and controlled by Analyst TF 1.7.1 software build 1163 (all AB Sciex, Framingham, MA, USA). In brief, peptides were dissolved in loading buffer (2% acetonitrile and 0.1% formic acid in water) to a concentration of 0.3 µg/µl. For each analysis, 1.5 µg protein was enriched on a self-packed precolumn (0.15 mm ID × 20 mm, Reprosil-Pur120 C18-AQ 5 µm, Dr. Maisch, Ammerbuch-Entringen, Germany) and separated on an analytical RP-C18

column (0.075 mm ID × 200 mm, Reprosil-Pur 120 C18-AQ, 3 µm, Dr. Maisch) with a 100 min linear gradient of 5–35% acetonitrile/0.1% formic acid (v:v) at 300 nl min^{-1}.

Samples were normalized to same protein amounts loaded onto the LC/MS/MS system prior to analysis and using a Total Area Sums approach following protein quantitation. Qualitative LC/MS/MS analysis was performed with a top 30 data-dependent acquisition method with an MS survey scan of *m/z* 380–1250 over 250 ms, at a resolution of 35000 full width at half maximum (FWHM). MS/MS scans of *m/z* 180–1500 were accumulated over 100 ms at a resolution of 17,500 FWHM and a precursor isolation width of 0.7 FWHM, thus resulting in a total cycle time of 3.4 s. Precursors above a threshold MS intensity of 200 cps with charge states of 2^+, 3^+ and 4^+ were selected for MS/MS. The dynamic exclusion time was set to 15 s. MS/MS activation was achieved by CID with nitrogen as a collision gas and the manufacturer's default rolling collision energy settings. Two biological replicates per sample were analyzed to construct a spectral library.

For quantitative SWATH analysis, MS/MS data were acquired with 100 variable size windows[20] across the 400–1200 *m/z* range. Fragments were produced with rolling collision energy settings for charge state 2^+, and fragments were acquired over an *m/z* range of 180–1500 for 40 ms per segment. Inclusion of a 250 ms survey scan resulted in an overall cycle time of 4.3 s. Two replicate injections were acquired for each of the two biological replicates of the four samples.

Protein identification was performed in ProteinPilot Software version 5.0 build 4304 (AB Sciex) with "thorough" settings. All MS/MS spectra from qualitative analyses were searched

against the UniProtKB Homo sapiens reference proteome (revision 01-2020) augmented with a set of 51 known common laboratory contaminants.

SWATH peak extraction was achieved in PeakView Software version 2.1 build 11041 (AB Sciex) with the SWATH quantification microApp version 2.0 build 2003. After retention time correction on endogenous peptides spanning the entire retention time range, peak areas were extracted with information from the MS/MS library.[21] The resulting peak areas were then summed to peptide and finally protein area values, which were used for further statistical analysis.

Multiplex-electrochemiluminescence assay

Frozen, undiluted samples were thawed and measured with a customized U-Plex assay (Meso Scale Discovery, Rockville, MD, USA) featuring three multiplex plates. Plate 1 contained TNF-α, IFN-γ, IL-1β, IL-10, IL-4, IL-13, IL-5, IL-8, IL-6, and MIP 3α; plate 2 contained IL-12/IL-23p40, TARC, MDC, MCP-1, MCP-4, Eotaxin, Eotaxin-3, MIP 1α, and MIP 1β; and plate 3 contained IL-31, TSLP, IL-22, IL-23, and IL-17A/F. Measurements were conducted on a MESO QuickPlex SQ 120 MM (Meso Scale Discovery) according to the manufacturer's instructions. One healthy control sample could not be analyzed. The detection limits can be found in the supplements (Table S1, Table S2).

scRNA-seq

Single cell RNA sequencing data from previous studies from five patients with AD, seven patients with PN and three healthy controls were used.[22] In addition, sequencing data from three patients with PSO were acquired via Gene Expression Omnibus (GSE162183).[23] For the AD, PN and healthy control samples, skin punch biopsies were dissolved with a skin dissociation kit from Miltenyi Biotech for cell isolation.

The isolated cells were immediately processed for single-cell RNA sequencing (scRNA-seq) with a Chromium Single Cell Controller and Single Cell 5′ Library & Gel Bead Kits from 10X Genomics, Pleasanton, CA, USA. The CellRanger pipeline version 6.1.2 was used for aligning the reads to the GRCH38 human reference genome. The expression matrix was loaded into the Seurat package version 4.3.0 for further downstream analyses. Cells with a high percentage of mitochondrial genes (> 12%) and either a very low (< 500) or a high number (> 6000) of unique genes (nFeature_RNA) were filtered out. Doublets were excluded with doubletFinder version 2.0.3. Integration via feature selection and identification of integration anchors was applied. The standard Seurat workflow was applied to process the samples, including principal component analysis (PCA) to identify 20 relevant dimensions through an elbow plot; subsequently, unsupervised clustering was performed with a resolution of 0.5. Cluster visualization was performed with Uniform Manifold Approximation and Projection (UMAP).

Statistical analyses

Statistical analysis of proteomics data

Data from the two available technical replicates were averaged for each biological replicate and used as representative values. PCA was performed on summed protein peak areas, and the first two principal components were visualized in a scatter plot. Groupwise multivariate t-distributions were fit to the principal components, and ellipses corresponding to the 95% quantiles were overlaid. Lesional samples were compared with nonlesional samples with paired t-tests and compared with control samples with Welch's t-test. The resulting p-values were adjusted for multiple testing with Benjamini-Hochberg correction to control for the false discovery rate. Standardized values of all proteins significantly differentially expressed in any pairwise comparison were displayed (as z-scores) in a clustered heatmap. Clustering of samples

and proteins was performed via hierarchical clustering with complete linkage and the Euclidian distance of the standardized expression profiles. Functional enrichment in Gene Ontology (GO) biological process terms and Kyoto Encyclopedia of Genes and Genomes (KEGG) pathways was assessed with gene set enrichment tests implemented in clusterProfiler (version 4.6.2).[24] The gene list was ordered by sign (test statistic) × (-$\log_{10}$(p value)). All gene sets with values between 10 and 500 were tested. The resulting enrichment scores and p values are reported. P-values were additionally adjusted for multiple testing with Benjamini-Hochberg correction to control for the false discovery rate.[25]

Statistical analysis of multiplex-electrochemiluminescence cytokine data

Calculations, graphs and comparisons between the lesional samples of each disease group and healthy control skin and between lesional and non-lesional samples within each disease were done on relative effects and tested for significance using the non-paired or paired version of the permutation-based Brunner-Munzel-Test[26] in R (version 4.2.1, R Foundation for Statistical Computing, Vienna, Austria). For statistical calculations, values below the determination range were set to zero.

Statistical analysis of single-cell RNA-seq data

The significance level was set to alpha = 5% for all statistical tests. All analyses were performed in R statistical software (version 4.2.1, R Foundation for Statistical Computing, Vienna, Austria). Benjamini-Hochberg correction was applied for analyses of single cell RNA sequencing data.

Results

Proteomics analysis of microdialysate reveals abnormalities in nonlesional skin of patients with AD

Mass spectrometry-based proteome profiling was performed on six participants with AD, seven with PSO, four with PN and seven healthy controls (Table 1). Across all samples, 793 proteins were identified, of which 702 were regularly quantified (Table S3). Volumes and total protein content of microdialysates did not differ significantly between the groups (Figure S3). After subtraction of proteins attributable to blood microparticles, according to their GO annotations, 517 proteins qualified for further analyses (Figure 1). Among the most differentially expressed gene products were oxysterol binding protein like 1A (OSBPL1A), serpins (SERPINB9 and SERPINA1), S100 proteins (S100A7A, S100A8, and S100A9), fatty acid binding proteins (FABP4, FABP5), and collagen (COL1A1) (Figure S4). PCA of the proteomics data indicated overlap of lesional and nonlesional samples from patients with AD and healthy control samples. In PN and PSO, the nonlesional samples overlapped with the control samples, whereas lesional samples showed a greater variation, with distinct principal components with respect to both nonlesional samples and healthy control samples (Figure 2a). We performed further investigation by hierarchical clustering of differentially abundant proteins in lesional skin, nonlesional skin and healthy control skin for all three diseases. For PSO and PN, lesional samples tended to cluster, whereas nonlesional samples overlapped with samples from healthy controls. For AD, no such clustering was observed (Figure 2b). Correlation of proteomic data with clinical parameters such as PASI/EASI or pruritus intensity did not reveal significant associations (data not shown).

We next analyzed differentially abundant proteins from groupwise comparisons for functional enrichment of the top 20 GO biological processes and KEGG pathways. Three of the top 20 enriched GO annotations (NAD metabolic process; regulation of secretion by cell; and pyruvate

metabolic process) overlapped between lesional AD vs. control skin, and lesional vs. nonlesional AD skin (Figure 3, Tables S4 and S5). Healthy control samples vs. lesional and vs. nonlesional AD samples shared only one of the top 20 enriched GO annotations (regulation of hormone levels; Tables S5 and S6). The KEGG pathways enriched between lesional and nonlesional AD skin almost completely overlapped with those in healthy control skin (Figure 3a, Tables S13–15). In PSO, six of the top 20 GO annotations were significantly overrepresented in lesional skin compared with both nonlesional skin and healthy control skin. The enriched terms included cellular response to stress (Figure 3, Tables S7 and S8). Correspondingly, 15 of 20 KEGG pathways were enriched in lesional skin compared with either nonlesional skin or healthy control skin (Tables S16–18). Nonlesional PSO skin was characterized by one overlapping GO annotation also present in lesional skin, but no KEGG pathways overlapped (Figure 3b, Tables S7–9, S16–18). Similar results were found for PN, for which five of the top 20 GO annotations were enriched in lesional skin compared with either nonlesional skin from the same patients or healthy control skin. In nonlesional PN skin vs healthy control skin, no GO annotation was significantly enriched with respect to lesional skin (Tables S10–12). Likewise, whereas five KEGG pathways were enriched in comparisons of lesional PN with either nonlesional PN or healthy control skin, no KEGG pathway was simultaneously enriched in nonlesional PN vs control skin and in lesional PN (Figure 3c, Tables S19–21).

Levels of extracellular cytokines IL12p40, IL-22, IL-8 and MCP-1 may be suitable disease markers

Most customized multiplex cytokine measurements of microdialysis samples were below the lower detection limit (full list of cytokines and corresponding values within the determination range in Table S2). IL12p40, IL-22, IL-8 and MCP-1 were widely identified in lesional skin of

diseased patients. In healthy controls, almost all cytokine measurements were below the detection limit. In patients with PSO, IL12p40 was significantly elevated in lesional skin compared with both nonlesional skin and healthy control skin (p=0.031 and p=0.009, Figure 4a). In AD and PN, IL12p40 abundance did not differ significantly. IL-22 was significantly elevated in lesional PSO skin compared with both nonlesional or healthy control skin (p=0.047 and p=0.001, respectively, Figure 4b). Again, no significant results were found for AD or PN. IL-8 was significantly elevated in PSO lesional skin compared with both nonlesional skin and healthy control skin (p=0.047 and p=0.001, respectively; Figure 4c). In AD, IL-8 was equally significantly elevated in lesional skin compared with both nonlesional and healthy control skin (p=0.031 and p=0.001, respectively). In PN, lesional skin significantly differed from healthy control skin (p=0.002) but not from nonlesional skin. MCP-1 was significantly elevated in skin lesions of patients with PSO compared with both nonlesional skin and healthy control skin (p=0.016 and p=0.001, Figure 4d). In AD, MCP-1 was significantly elevated in lesional skin only when compared to healthy control skin (p=0.005) but not to nonlesional skin. Again, no significant differences were found in the samples of patients with PN. TSLP was elevated, although not statistically significantly, in lesions of three patients with PSO, but was below the detection limit in corresponding nonlesional samples (Figure S5). Individual samples contained IL-1β, MCP-4 or MDC, but their patient sample size with positive results was too low to yield statistically relevant results (Figures S6–8).

Identical cellular origin of cytokines in AD, PSO and PN in integrated single-cell RNA-seq data from skin biopsies

Single-cell RNA sequencing data revealed that *CCL2* (MCP-1) was produced by various cells including endothelial cells, fibroblasts, epithelial cells and smooth muscle cells (Figure 5). *CXCL8* (IL-8) was produced primarily by antigen-presenting cells in diseased and healthy

participants. We observed no evidence of IL22 transcripts in single-cell RNA sequencing data of healthy individuals. In AD, PN and PSO, IL22 originated from lymphocytes. IL12B was not detected via RNA-seq.

Discussion

The main goal of this study was to assess skin microdialysis as a diagnostic tool for profiling various inflammatory skin diseases. We identified patterns associated with the investigated diseases. Our findings suggest that pathophysiological changes in PSO and PN are limited to the inflammatory lesions, whereas skin alterations in patients with AD also affect nonlesional, non-inflamed skin. These data are consistent with previous research findings indicating that hallmarks of AD inflammation occur before, and persists after, clinically visible inflammation has subsided.[11,27–29]

The second focus of this study was to identify unique protein disease profiles locally in skin lesions through comparisons of skin from patients with AD, PSO or PN versus healthy control skin. Using microdialysis, we found oxysterol-binding protein-related protein 1 (OSBPL1A) expression was more than tenfold higher in AD compared to PN. Previous research found it decreased in PSO.[30] Contrary to this, alpha-1 type I collagen (COL1A1) was more than three-fold increased in PN compared to AD or healthy control skin, reflecting fibrotic processes and previous findings from single cell analyses.[22] We detected 7-to-23-fold increased levels of S100 proteins type A7, A8, and A9 in PSO compared to healthy control skin, as expected from other methods.[30] In PN, protease inhibitors of the serpin family were downregulated, while serpin B9 was upregulated more than 5-fold in PSO. In all three diseases, fatty acid binding protein (FABP) 5 was upregulated at the expense of FABP 4, which was downregulated.

In our study, comparisons of cytokine expression profiles were not possible through proteomics analyses, because the resolution of our proteomics approach was insufficient to detect many known cytokines, despite the above-mentioned sample processing steps. Of note, other methods of in situ transcriptome and proteome analyses also did not register elevated levels of already known central disease mediators in lesional skin, for example IL-17 or IL-23.[31,32] Furthermore, performing microdialysis on inflamed skin often yielded blood-contaminated

dialysates. Visible blood contamination was most prominent in PSO and PN lesions and was mostly absent in nonlesional skin and healthy control skin. Therefore, we subtracted proteins attributable to blood microparticles in our statistical analysis. However, blood contamination due to microlesions seems an inherent problem with this method for analyses of skin with high vascularization, such as PSO skin.

Consequently, we performed protein analyses with the microdialysates by highly sensitive electrochemiluminescence assays. Most assayed cytokines were below the detection limit, possibly because we used the second collection vial obtained during microdialysis. Relevant amounts of cytokines might have been washed out during the first 20 minutes, thus resulting in a lower protein concentration in the second collection vial. Key factors determining the protein concentration in the dialysate are rate of release, binding to high affinity receptors in tissue[33] and the diffusion rate in the tissue toward the dialysis membrane, which is lower for larger proteins. Indeed, upregulation of IL4R on fibroblasts in AD has been demonstrated by single cell transcriptomics[34] and therefore upregulation of receptors might have decreased cytokine availability at the microdialysis catheter. We already attempted to account for low protein concentrations by using an assay with high sensitivity (electrochemiluminescence) requiring small sample sizes. This process enabled us to analyze all cytokines without dilution. The cytokines yielding statistically relevant results included IL-12B, IL-22, CXCL8 and MCP-1. Previous research indicated that IL12B (equivalent to IL-12p40) and IL-1β can be used as biomarkers to guide PSO therapy[35], and IL-12B can be used to predict disease progression.[36] We found that IL-12p40 was specifically enriched in PSO lesions, and we verified the presence of IL-1β in some of the PSO samples, thus validating our measurements. We further observed MCP-1 (CCL2) elevation in PSO lesions compared with nonlesional or healthy control skin, and in AD samples compared with healthy control samples. MCP-1 is a monocyte chemoattractant protein secreted by various cells including keratinocytes. Its receptor, CCR2,

is expressed on the surfaces of monocytes, and MCP-1 levels are elevated in PSO, AD and other skin disorders,[37] and show broad upregulation in fibroblasts, keratinocytes and pericytes,[34] in agreement with our findings. CXCL8 (IL-8), a chemoattractant for neutrophils, is secreted primarily by antigen-presenting cells. In inflammatory conditions, IL-8 may also be secreted by keratinocytes after stimulation with IL-17A, and its expression is regulated by IL-36, among other cytokines.[32-34] Correspondingly, in accordance with previous literature,[41] CXCL8 was elevated in lesional samples of all three diseases studied here. Little research has described the role of CXCL8 in PN. One recent study has indicated CXCL8 elevation in PN lesions compared with AD lesions through transcriptomic analysis.[42] To our knowledge, this study reports the first data on lesional IL-8 protein levels. In accordance with previous research, we found that IL-8 levels were elevated in lesional skin of both AD and PN. However, we were unable to confirm higher levels in PN lesions than AD lesions, thus extending previous results.[42] Most cytokines were scarce in our PN samples, and statistically significant differences were rarely observed, possibly because of an insufficient number of patients with PN or because extracellular cytokine levels are generally lower in PN than in other diseases such as PSO. Furthermore, IL-22, originating from lymphocytes, was elevated in cytokine measurements of PSO. Greater IL-22 levels in PSO than in healthy control skin were expected, according to the current pathophysiological understanding of the disease.[43] These considerations demonstrated the integrity of our data. Unfortunately, none of the observed parameters could serve as a novel biomarker to distinguish the three diseases or support disease classification. Furthermore, proteomics may not be an ideal tool to detect cytokines, and other tools might be necessary, such as transcriptomics and ELISA. Although extracellular cytokine levels should reflect the type and acuity of inflammatory responses most accurately, paracrine and autocrine signaling combined with an extensive capacity of high affinity receptors might critically decrease the spillover captured by the microdialysis membrane. Thus, the integrated

approach of microdialysis combined with scRNA-seq appears promising. Further research may combine these techniques within the same patient and additionally focus on the poorly understood role of CXCL8 in PN.

The main limitation of this study is its small sample size. The sample size did not allow differentiating different disease severities or other clinical features of the analyzed lesions. In future studies, including different molecular subtypes of AD, such as type 2 high and type 2 low AD, might be beneficial, because these subtypes differ in their cytokine expression profiles.[6] Nummular eczema has been suggested to be a variant of AD with a codominant Th2/Th17 immune response; therefore, the researched diseases might have broad and partly overlapping cytokine expression profiles.[44] Such overlap was reflected in our data. In addition, some patients with AD may have high IL-31 levels.[45] Lesional skin of different patients with AD did not cluster well, in contrast to samples from patients with PSO. Not only disease subtypes but also the timing of the microdialysis procedure may influence the results. Inflammatory lesions undergo transformation over time. Type 3 immune responses, as seen in PSO, for example, show high plasticity. Over time, type 3 related cells shift toward IFN-γ production, away from type 3 immunity.[2] Disease endotypes and time-dependent plasticity might explain why certain cytokines, such as thymic stromal lymphopoietin (TSLP), were elevated in lesions in only some of our patients. Keratinocyte-derived TSLP is a prominent protein inducing Th2 polarization via DCs in the skin.[46] However, TSLP has been found to be elevated in PSO and associated with its pathophysiology.[41-43] This finding may also explain the failure of clinical trials of an antibody to TSLP for treatment of AD.

In conclusion, microdialysis is a promising method through which lesional and nonlesional skin samples can be analyzed, even repetitively. This method yields fluids that can be used for proteomics analyses and protein measurements. However, we did not find evidence that microdialysis can easily differentiate inflammation profiles of different skin diseases. *CXCL8*

492 is elevated in PN, a finding not previously reported. In PN and PSO, inflammation may be
493 limited to lesional skin, whereas in AD, nonlesional skin shows characteristics of lesional skin.
494 Thus, microdialysis may serve as a valuable tool for further understanding the pathophysiology
495 of chronic inflammatory skin diseases.
496

497 **Acknowledgements**

498 We acknowledge excellent technical support by Meike Schaffrinski. The graphical abstract
499 was created using BioRender.com
500

References

1. Lauffer F, Jargosch M, Krause L, Garzorz-Stark N, Franz R, Roenneberg S, et al. Type I Immune Response Induces Keratinocyte Necroptosis and Is Associated with Interface Dermatitis. J Invest Dermatol. 2018 Aug;138(8):1785–94.

2. Annunziato F, Romagnani C, Romagnani S. The 3 major types of innate and adaptive cell-mediated effector immunity. J Allergy Clin Immunol. 2015 Mar;135(3):626–35.

3. Ständer S. Atopic Dermatitis. Ropper AH, editor. N Engl J Med. 2021 Mar 25;384(12):1136–43.

4. Treudler R, Simon J. Developments and perspectives in allergology. JDDG J Dtsch Dermatol Ges. 2023 Apr;21(4):399–403.

5. Gieseck RL, Wilson MS, Wynn TA. Type 2 immunity in tissue repair and fibrosis. Nat Rev Immunol. 2018 Jan;18(1):62–76.

6. Akdis CA, Arkwright PD, Brüggen MC, Busse W, Gadina M, Guttman-Yassky E, et al. Type 2 immunity in the skin and lungs. Allergy. 2020 Jul;75(7):1582–605.

7. Schön MP, Berking C, Biedermann T, Buhl T, Erpenbeck L, Eyerich K, et al. COVID-19 and immunological regulations - from basic and translational aspects to clinical implications. JDDG J Dtsch Dermatol Ges. 2020 Aug;18(8):795–807.

8. Czarnowicki T, He H, Krueger JG, Guttman-Yassky E. Atopic dermatitis endotypes and implications for targeted therapeutics. J Allergy Clin Immunol. 2019 Jan;143(1):1–11.

9. Schäbitz A, Eyerich K, Garzorz-Stark N. So close, and yet so far away: The dichotomy of the specific immune response and inflammation in psoriasis and atopic dermatitis. J Intern Med. 2021 Jul;290(1):27–39.

10. Lauffer F, Eyerich K. Eczematized psoriasis - a frequent but often neglected variant of plaque psoriasis. J Dtsch Dermatol Ges J Ger Soc Dermatol JDDG. 2023 May;21(5):445–53.

11. Brunner PM, Emerson RO, Tipton C, Garcet S, Khattri S, Coats I, et al. Nonlesional atopic dermatitis skin shares similar T-cell clones with lesional tissues. Allergy. 2017 Dec;72(12):2017–25.

12. Langan SM, Irvine AD, Weidinger S. Atopic dermatitis. The Lancet. 2020 Aug;396(10247):345–60.

13. Steinhoff M, Ahmad F, Pandey A, Datsi A, AlHammadi A, Al-Khawaga S, et al. Neuroimmune communication regulating pruritus in atopic dermatitis. J Allergy Clin Immunol. 2022 Jun;149(6):1875–98.

14. Agelopoulos K, Renkhold L, Wiegmann H, Dugas M, Süer A, Zeidler C, et al. Transcriptomic, Epigenomic, and Neuroanatomic Signatures Differ in Chronic Prurigo, Atopic Dermatitis, and Brachioradial Pruritus. J Invest Dermatol. 2023 Feb;143(2):264-272.e3.

15. Garzorz-Stark N, Krause L, Lauffer F, Atenhan A, Thomas J, Stark SP, et al. A novel molecular disease classifier for psoriasis and eczema. Exp Dermatol. 2016 Oct;25(10):767–74.

16. Schmelz M, Luz O, Averbeck B, Bickel A. Plasma extravasation and neuropeptide release in human skin as measured by intradermal microdialysis. Neurosci Lett. 1997 Jul;230(2):117–20.

17. Baumann KY, Church MK, Clough GF, Quist SR, Schmelz M, Skov PS, et al. Skin microdialysis: methods, applications and future opportunities—an EAACI position paper. Clin Transl Allergy. 2019 Dec;9(1):24.

18. Papoiu ADP, Wang H, Nattkemper L, Tey HL, Ishiuji Y, Chan YH, et al. A study of serum concentrations and dermal levels of NGF in atopic dermatitis and healthy subjects. Neuropeptides. 2011 Dec;45(6):417–22.

19. Hughes CS, Moggridge S, Müller T, Sorensen PH, Morin GB, Krijgsveld J. Single-pot, solid-phase-enhanced sample preparation for proteomics experiments. Nat Protoc. 2019 Jan;14(1):68–85.

20. Zhang Y, Bilbao A, Bruderer T, Luban J, Strambio-De-Castillia C, Lisacek F, et al. The Use of Variable Q1 Isolation Windows Improves Selectivity in LC-SWATH-MS Acquisition. J Proteome Res. 2015 Oct 2;14(10):4359–71.

21. Lambert JP, Ivosev G, Couzens AL, Larsen B, Taipale M, Lin ZY, et al. Mapping differential interactomes by affinity purification coupled with data-independent mass spectrometry acquisition. Nat Methods. 2013 Dec;10(12):1239–45.

22. Alkon N, Assen FP, Arnoldner T, Bauer WM, Medjimorec MA, Shaw LE, et al. Single-cell RNA sequencing defines disease-specific differences between chronic nodular prurigo and atopic dermatitis. J Allergy Clin Immunol. 2023 Aug;152(2):420–35.

23. Gao Y, Yao X, Zhai Y, Li L, Li H, Sun X, et al. Single cell transcriptional zonation of human psoriasis skin identifies an alternative immunoregulatory axis conducted by skin resident cells. Cell Death Dis. 2021 May 6;12(5):450.

24. Yu G, Wang LG, Han Y, He QY. clusterProfiler: an R package for comparing biological themes among gene clusters. Omics J Integr Biol. 2012 May;16(5):284–7.

25. Subramanian A, Tamayo P, Mootha VK, Mukherjee S, Ebert BL, Gillette MA, et al. Gene set enrichment analysis: A knowledge-based approach for interpreting genome-wide expression profiles. Proc Natl Acad Sci. 2005 Oct 25;102(43):15545–50.

26. Pauly M, Asendorf T, Konietschke F. Permutation-based inference for the AUC: A unified approach for continuous and discontinuous data. Biom J. 2016 Nov;58(6):1319–37.

27. Sirvent S, Vallejo AF, Corden E, Teo Y, Davies J, Clayton K, et al. Impaired expression of metallothioneins contributes to allergen-induced inflammation in patients with atopic dermatitis. Nat Commun. 2023 May 19;14(1):2880.

28. Pavel AB, Renert-Yuval Y, Wu J, Del Duca E, Diaz A, Lefferdink R, et al. Tape strips from early-onset pediatric atopic dermatitis highlight disease abnormalities in nonlesional skin. Allergy. 2021 Jan;76(1):314–25.

29. Suárez-Fariñas M, Tintle SJ, Shemer A, Chiricozzi A, Nograles K, Cardinale I, et al. Nonlesional atopic dermatitis skin is characterized by broad terminal differentiation defects and variable immune abnormalities. J Allergy Clin Immunol. 2011 Apr;127(4):954-964.e4.

30. Rioux G, Simard M, Morin S, Lorthois I, Guérin SL, Pouliot R. Development of a 3D psoriatic skin model optimized for infiltration of IL-17A producing T cells: Focus on the crosstalk between T cells and psoriatic keratinocytes. Acta Biomater. 2021 Dec;136:210–22.

31. Frost B, Schmidt M, Klein B, Loeffler-Wirth H, Krohn K, Reidenbach T, et al. Single-cell transcriptomics reveals prominent expression of IL-14, IL-18, and IL-32 in psoriasis. Eur J Immunol. 2023 Nov;53(11):2250354.

32. Schäbitz A, Hillig C, Mubarak M, Jargosch M, Farnoud A, Scala E, et al. Spatial transcriptomics landscape of lesions from non-communicable inflammatory skin diseases. Nat Commun. 2022 Dec 13;13(1):7729.

33. Thurley K, Gerecht D, Friedmann E, Höfer T. Three-Dimensional Gradients of Cytokine Signaling between T Cells. PLoS Comput Biol. 2015 Apr;11(4):e1004206.

34. He H, Suryawanshi H, Morozov P, Gay-Mimbrera J, Del Duca E, Kim HJ, et al. Single-cell transcriptome analysis of human skin identifies novel fibroblast subpopulation and enrichment of immune subsets in atopic dermatitis. J Allergy Clin Immunol. 2020 Jun;145(6):1615–28.

35. Corbett M, Ramessur R, Marshall D, Acencio ML, Ostaszewski M, Barbosa IA, et al. Biomarkers of systemic treatment response in people with psoriasis: a scoping review. Br J Dermatol. 2022 Oct;187(4):494–506.

36. Ramessur R, Corbett M, Marshall D, Acencio ML, Barbosa IA, Dand N, et al. Biomarkers of disease progression in people with psoriasis: a scoping review. Br J Dermatol. 2022 Oct;187(4):481–93.

37. Behfar S, Hassanshahi G, Nazari A, Khorramdelazad H. A brief look at the role of monocyte chemoattractant protein-1 (CCL2) in the pathophysiology of psoriasis. Cytokine. 2018 Oct 1;110:226–31.

38. Furue M, Kadono T. "Inflammatory skin march" in atopic dermatitis and psoriasis. Inflamm Res. 2017 Oct 1;66(10):833–42.

39. Nedoszytko B, Sokołowska-Wojdyło M, Ruckemann-Dziurdzińska K, Roszkiewicz J, Nowicki R. Chemokines and cytokines network in the pathogenesis of the inflammatory skin diseases: atopic dermatitis, psoriasis and skin mastocytosis. Adv Dermatol Allergol Dermatol Alergol. 2014;31(2):84–91.

40. Ogawa E, Sato Y, Minagawa A, Okuyama R. Pathogenesis of psoriasis and development of treatment. J Dermatol. 2018;45(3):264–72.

41. Zhou Z, Meng L, Cai Y, Yan W, Bai Y, Chen J. Exploration of the Potential Mechanism of the Common Differentially Expressed Genes in Psoriasis and Atopic Dermatitis. BioMed Res Int. 2022 May 9;2022:1177299.

42. Deng J, Parthasarathy V, Marani M, Bordeaux Z, Lee K, Trinh C, et al. Extracellular matrix and dermal nerve growth factor dysregulation in prurigo nodularis compared to atopic dermatitis. Front Med. 2022 Dec 21;9:1022889.

43. Boehncke WH, Schön MP. Psoriasis. The Lancet. 2015 Sep;386(9997):983–94.

44. Böhner A, Jargosch M, Müller NS, Garzorz-Stark N, Pilz C, Lauffer F, et al. The neglected twin: nummular eczema is a variant of atopic dermatitis with co-dominant Th2/Th17 immune response. J Allergy Clin Immunol. 2023 Apr;S0091674923005146.

45. Cevikbas F, Wang X, Akiyama T, Kempkes C, Savinko T, Antal A, et al. A sensory neuron-expressed IL-31 receptor mediates T helper cell-dependent itch: Involvement of TRPV1 and TRPA1. J Allergy Clin Immunol. 2014 Feb;133(2):448–60.

46. Traidl S, Roesner L, Zeitvogel J, Werfel T. Eczema herpeticum in atopic dermatitis. Allergy. 2021 Oct;76(10):3017–27.

47. Li SZ, Jin XX, Shan Y, Jin HZ, Zuo YG. Expression of Thymic Stromal Lymphopoietin in Immune-Related Dermatoses. Mediators Inflamm. 2022 Aug 21;2022:9242383.

48. Suwarsa O, Dharmadji HP, Sutedja E, Herlina L, Sori PR, Hindritiani R, et al. Skin tissue expression and serum level of thymic stromal lymphopoietin in patients with psoriasis vulgaris. Dermatol Rep [Internet]. 2019 Jun 20 [cited 2023 Jun 13];11(1). Available from: https://www.pagepress.org/journals/index.php/dr/article/view/8006

49. Volpe E, Pattarini L, Martinez-Cingolani C, Meller S, Donnadieu MH, Bogiatzi SI, et al. Thymic stromal lymphopoietin links keratinocytes and dendritic cell–derived IL-23 in patients with psoriasis. J Allergy Clin Immunol. 2014 Aug 1;134(2):373-381.e4.

641 **Table**

642

Participant	Age	DLQI	VAS10 (Itch)	Score	Proteomics	MSD
Atopic dermatitis (AD, n = 6)				EASI		
AD (1)	36	16	8,5	34,9	yes	yes
AD (2)	79	8	2	13,4	yes	yes
AD (3)	60	15	2	18,5	yes	yes
AD (4)	24	11	6	14,6	yes	yes
AD (5)	21	11	0	16,6	yes	yes
AD (6)	24	8	6	4,8	yes	yes
Psoriasis vulgaris (PSO, n = 7)				PASI		
PSO (1)	60	15	8	24,8	yes	yes
PSO (2)	55	23	8	22,1	yes	yes
PSO (3)	38	29	10	20,9	yes	yes
PSO (4)	54	23	3	5,1	yes	yes
PSO (5)	64	14	5,5	10,1	yes	yes
PSO (6)	73	13	6	4,8	yes	yes
PSO (7)	28	-	6	14,6	yes	yes
Prurigo nodularis (PN, n = 6)						
PN (1)	62	12	6		yes	yes
PN (2)	70	7	7		yes	yes
PN (3)	66	7	8		yes	yes
PN (4)	57	22	8,5		yes	yes
PN (5)	62	18	7		-	yes
PN (6)	82	10	7		-	yes
Controls (C, n = 7)						
C (1)	42	1	0		yes	yes
C (2)	51	0	0		yes	yes
C (3)	47	1	2		yes	yes
C (4)	25	0	0		yes	yes
C (5)	34	0	1		yes	yes
C (6)	71	0	0		yes	yes
C (7)	37	0	0		yes	-

643 Table 1: Patient characteristics

644 **Figure Legends**

645

646 Fig. 1.

647 **Outline.** Recruited participants with their respective condition are depicted at the top. Below
648 are the processes of proteomic (left) and multiplex-electrochemiluminescence (right)
649 analyses.

650

651 Fig. 2.

652 **Lesional skin in psoriasis vulgaris (PSO, n=7) and prurigo nodularis (PN, n=4) but not in**
653 **atopic dermatitis (AD, n=6) differs from nonlesional skin and skin of healthy controls**
654 **(n=7).** (a) Shows the proteomics data visualized through principal component analysis (PCA)
655 and ellipses corresponding to the 95% quantiles of fitted groupwise multivariate t-distributions.
656 Grey depicts controls, red represents AD, lilac illustrates PSO and PN was colored green. In
657 each PCA, the darker color represents lesional skin whereas the lighter color symbolizes
658 nonlesional skin. (b) Shows a heatmap of a hierarchical clustering encompassing all values that
659 are significantly differing between lesional, nonlesional and/or control skin for AD (left), PSO
660 (middle) and PN (right). In the hierarchical clustering, black depicts lesional skin, white
661 represents nonlesional skin and grey represents the healthy controls. The z-value is visualized
662 on a continuous color scale from blue (-4) via white (0) to red (4).

663

664 Fig. 3.

665 **Proteins overexpressed in lesional skin vs nonlesional skin overlap in enriched GO**
666 **annotations and KEGG pathways with lesional skin vs healthy controls in both psoriasis**
667 **vulgaris (PSO) and prurigo nodularis (PN).** Groupwise comparisons of lesional vs
668 nonlesional, lesional vs control as well as nonlesional vs control samples from the proteomics
669 data. Significantly over- or underexpressed proteins in these comparisons were analyzed with
670 regard to overlaps in their top 20 enriched GO annotations (left) and top 20 enriched KEGG
671 pathways (right) and visualized in Euler diagrams.

672

673 Fig. 4.

674 **IL-22 and MCP-1 measured by electrochemiluminescence assay are overexpressed in**
675 **PSO lesional skin vs nonlesional skin (n=7) and vs healthy controls (n=6) but not in**
676 **lesional vs nonlesional AD (n=6) or PN (n=6) skin.** (a) IL-12p40, (b) IL-22 (c) IL-8 and (d)

MCP-1 graphs per disease group and subcategorized into lesional (L) and nonlesional (nL) skin. Comparisons between the L samples of each disease group and controls and between L and nL samples within each disease were done on relative effects and tested for significance using the non-paired or the paired version of the permutation-based Brunner-Munzel-Test: **p < 0.01; *p < 0.05.

Fig. 5.

Single cell RNAseq data revealed that Il-22 originated from lymphocytes and IL-8 originated from antigen-presenting cells. (a) Uniform Manifold Approximation and Projection for Dimension Reduction (UMAP) plot (140363 cells) of integrated single-cell RNA sequencing data. Based on differential expressed genes multiple cell cluster were identified: T cells (T1, T2), NK cells, antigen-presenting cells (DC1,DC2), mast cells (MC), melanocytes (MEL), smooth muscle cells (SCM1, SMC2), blood vascular endothelial cells (BEC1, BEC2, BEC3), lymphatic endothelial cells (LEC), fibroblasts (FB1, FB2, FB3, proliferative FB [FBpro]), sebaceous gland cells (SG), Keratinocytes (KC1, KC2, KC3, KC3, KC5, proliferative KC [KCpro]). Feature plot of proliferating cells marked by MKI67 expression. (b) Dot plot of the hallmark transcripts expressed by the identified clusters. (c) Bar chart depicting the relative proportion of cells from each disease in every cluster. (red = atopic dermatitis [AD] (n=5), blue = psoriasis vulgaris [PSO] (n=3), orange = prurigo nodularis [PN] (n=7), grey = control [C]) (n=3) (d) Feature plots showing the MCP-1 (CCL2), Il-8 (CXCL8), IL-22, and IL-12p40 (IL-12B) producing cells in healthy controls, AD, PN, and PSO.

Hollstein et al. Figure 1

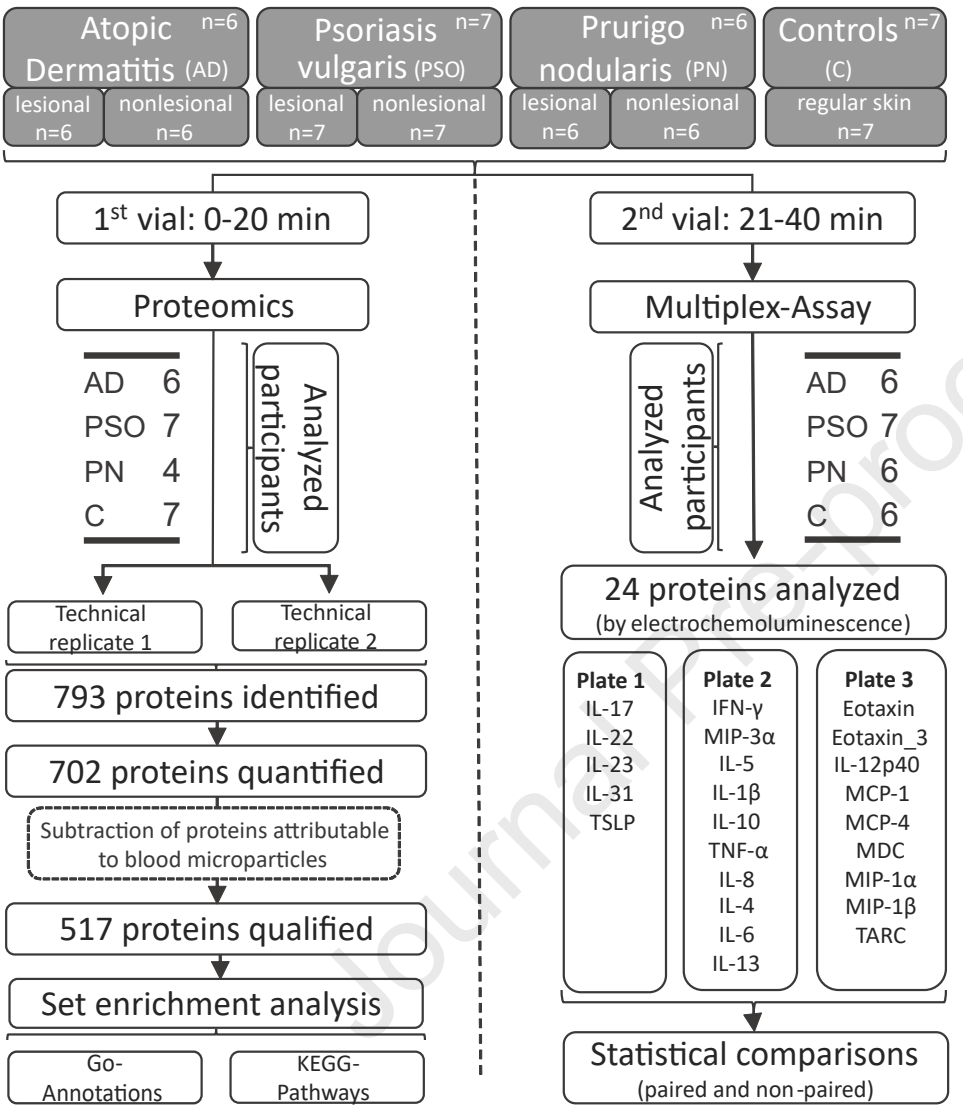

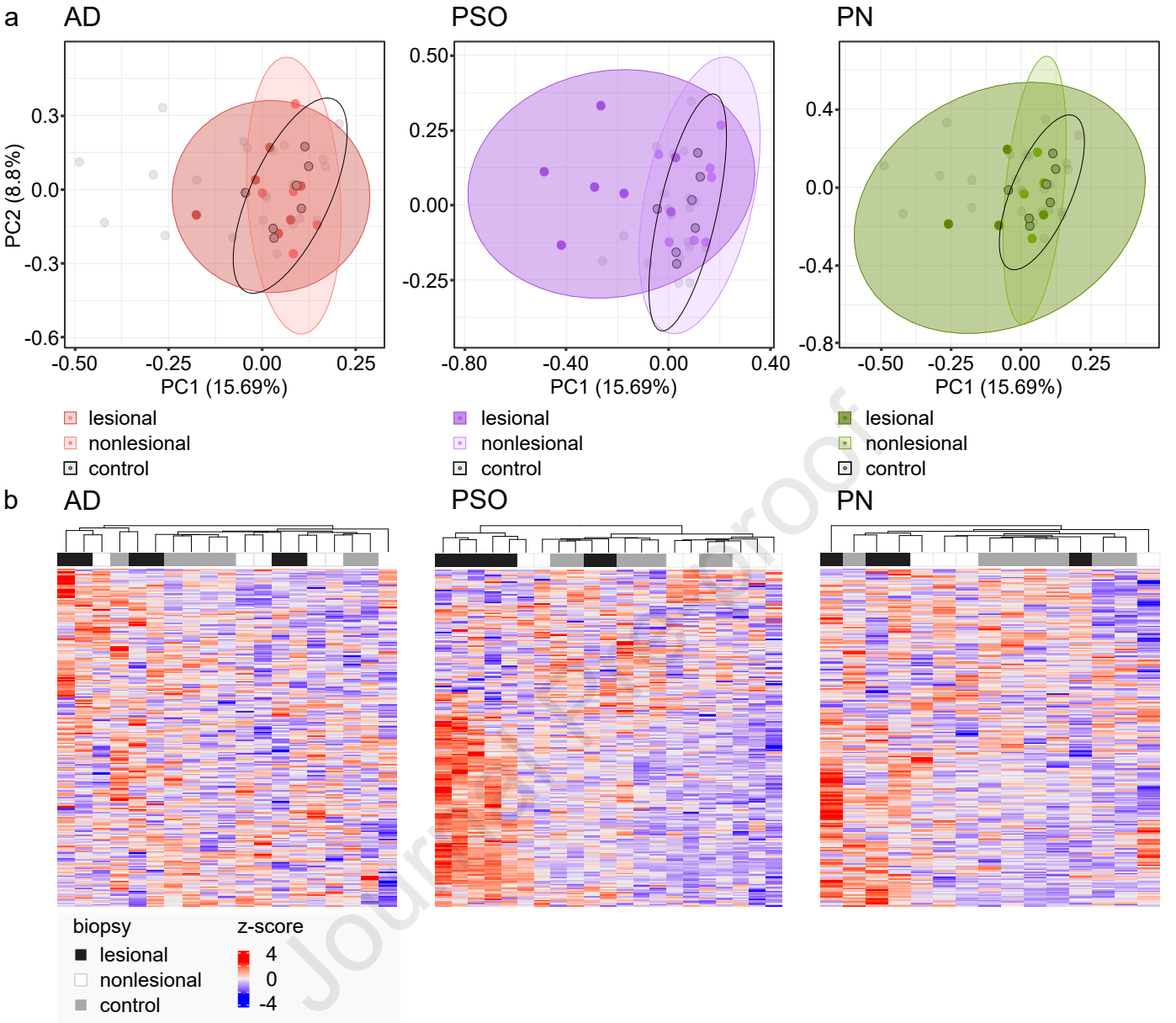

a AD

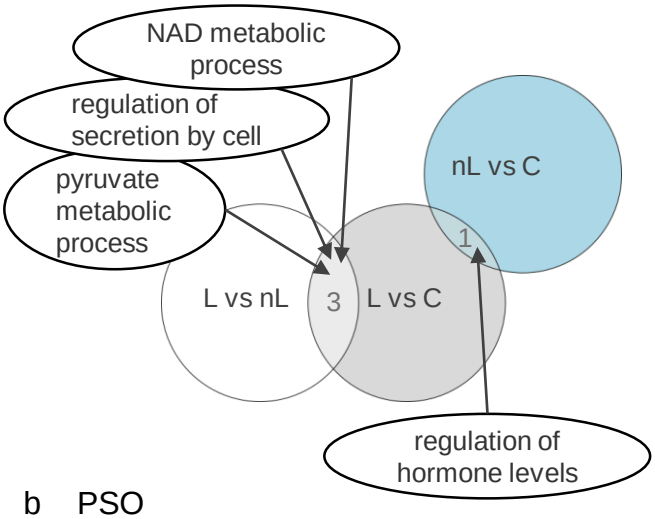

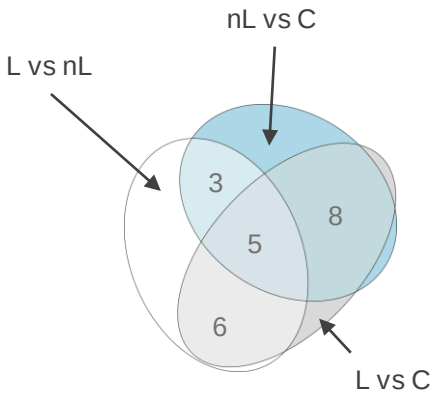

b PSO

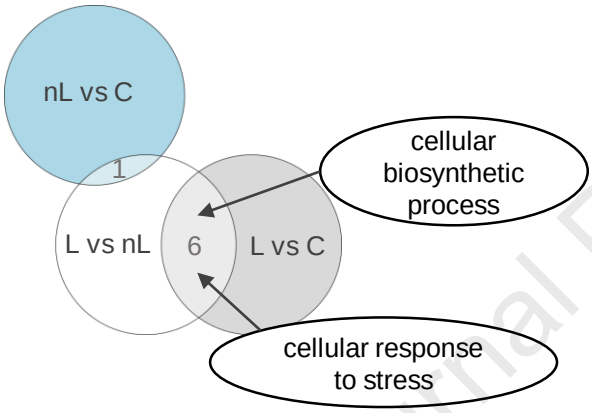

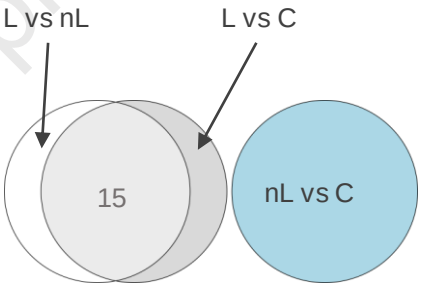

c PN

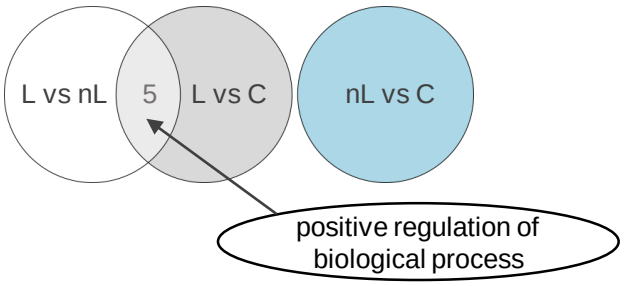

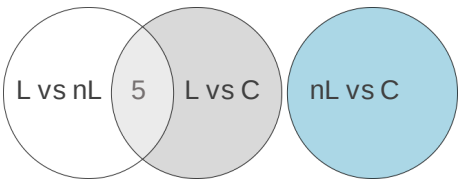

Top 20 GO-Annotations

Top 20 KEGG-Pathways

Hollstein et al. Figure 4